

# Metamagnetic transition in $\text{EuFe}_2\text{As}_2$ single crystals

Shuai Jiang, Yongkang Luo, Zhi Ren, Zengwei Zhu, Cao Wang,  
Xiangfan Xu, Qian Tao, Guanghan Cao<sup>†</sup>, and Zhu'an Xu<sup>‡</sup>

Department of Physics, Zhejiang University, Hangzhou 310027, People's Republic of China

E-mail: <sup>†</sup>ghcao@zju.edu.cn; <sup>‡</sup>zhuan@zju.edu.cn

**Abstract.** We report the measurements of anisotropic magnetization and magnetoresistance on single crystals of  $\text{EuFe}_2\text{As}_2$ , a parent compound of ferro-arsenide high-temperature superconductor. Apart from the antiferromagnetic (AFM) spin-density-wave transition at 186 K associated with Fe moments, the compound undergoes another magnetic phase transition at 19 K due to AFM ordering of  $\text{Eu}^{2+}$  spins ( $J = S = 7/2$ ). The latter AFM state exhibits metamagnetic transition under magnetic fields. Upon applying magnetic field with  $H \parallel c$  at 2 K, the magnetization increases linearly to  $7.0 \mu_B/\text{f.u.}$  at  $\mu_0 H = 1.7$  T, then keeps at this value of saturated  $\text{Eu}^{2+}$  moments under higher fields. In the case of  $H \parallel ab$ , the magnetization increases step-like to  $6.6 \mu_B/\text{f.u.}$  with small magnetic hysteresis. A metamagnetic phase was identified with the saturated moments of  $4.4 \mu_B/\text{f.u.}$  The metamagnetic transition accompanies with negative in-plane magnetoresistance, reflecting the influence of  $\text{Eu}^{2+}$  moments ordering on the electrical conduction of FeAs layers. The results were explained in terms of spin-reorientation and spin-reversal based on an *A*-type AFM structure for  $\text{Eu}^{2+}$  spins. The magnetic phase diagram has been established.

PACS numbers: 74.10.+v; 75.30.Kz; 75.30.Cr; 75.47.Pq

## 1. Introduction

The discovery of high temperature superconductivity in  $\text{LnFeAsO}_{1-x}\text{F}_x$  (Ln=lanthanides)[1, 2, 3] has stimulated intense research in the field of condensed matter physics. The superconducting transition temperature has achieved 55 K or more by either high-pressure synthesis[4, 5] or Th-doping strategy[6]. The key structural unit of the superconductors is accepted as the antiferroite-type  $[\text{Fe}_2\text{As}_2]^{2-}$  layers. This point of view is manifested by the observation of superconductivity up to  $\sim 38$  K in  $\text{Ba}_{1-x}\text{K}_x\text{Fe}_2\text{As}_2$ [7],  $\text{Sr}_{1-x}\text{K}_x\text{Fe}_2\text{As}_2$ [8, 9],  $\text{Ca}_{1-x}\text{Na}_x\text{Fe}_2\text{As}_2$ [10], and  $\text{Li}_{1-x}\text{FeAs}$ [11], all of which contain similar  $[\text{Fe}_2\text{As}_2]^{2-}$  layers. Another important point is that the Fe sublattice of the parent compound is antiferromagnetic (AFM) in the ground state[12, 13], and superconductivity is induced by suppressing the AFM order through appropriate carrier doping.

$\text{EuFe}_2\text{As}_2$ [14] belongs to the so-called "122" family  $A\text{Fe}_2\text{As}_2$  ( $A=\text{Ba}, \text{Sr}, \text{Ca}$  and  $\text{Eu}$ ), and it stands out due to the magnetic moments of  $\text{Eu}^{2+}$ . We have recently performed a systematic physical property measurements on  $\text{EuFe}_2\text{As}_2$  polycrystalline sample.[15] Very similar magnetic transition related to  $\text{Fe}_2\text{As}_2$  layers was revealed between  $\text{EuFe}_2\text{As}_2$  and  $\text{SrFe}_2\text{As}_2$ . By assuming that  $\text{Eu}^{2+}$  moments are compatible with superconductivity, we had anticipated that superconductivity might be realized by proper doping in  $\text{EuFe}_2\text{As}_2$  systems. As a matter of fact, superconductivity was indeed obtained in  $\text{Eu}_{0.5}\text{K}_{0.5}\text{Fe}_2\text{As}_2$  and  $\text{Eu}_{0.7}\text{Na}_{0.3}\text{Fe}_2\text{As}_2$ , according to very recent reports[16, 17].

Although the free  $\text{Eu}^{2+}$  moments do not directly affect superconductivity, study on the ordering of  $\text{Eu}^{2+}$  moments may shed light on the mechanism of high-temperature superconductivity in iron arsenides. Our preceding work[15] indicated that the magnetic ordering of  $\text{Eu}^{2+}$  moments in  $\text{EuFe}_2\text{As}_2$  was very intriguing. While the  $\text{Eu}^{2+}$  spins ( $S=7/2, L=0$ ) order antiferromagnetically below 19 K at zero field, the Curie-Weiss fit of high-temperature magnetic susceptibility suggests ferromagnetic interactions between the  $\text{Eu}^{2+}$  spins. When applying magnetic field, a metamagnetic transition was found around 0.65 T. To further understand the intrinsic properties of this magnetically ordered materials, we performed the measurements of anisotropic magnetization and magnetoresistance on single crystals of  $\text{EuFe}_2\text{As}_2$ . As a result, anisotropic metamagnetic transitions were uncovered. What is more, the electrical conduction of FeAs layers was found to be related to the magnetic state of Eu layers.

## 2. Experimental details

Single crystals of  $\text{EuFe}_2\text{As}_2$  were grown using FeAs as the self-flux similar to previous report[18]. FeAs was presynthesized by reacting Fe powders with As shots in vacuum at 773 K for 6 hours and then 1030 K for 12 hours. Fresh Eu grains and FeAs powders were thoroughly mixed in a molar ratio of 1:4. The mixture was loaded into an alumina tube which was put into a quartz ampoule. The sealed quartz ampoule was heated to 1053 K at a rate of 150 K/h, holding for 10 hours. Subsequently, the temperature

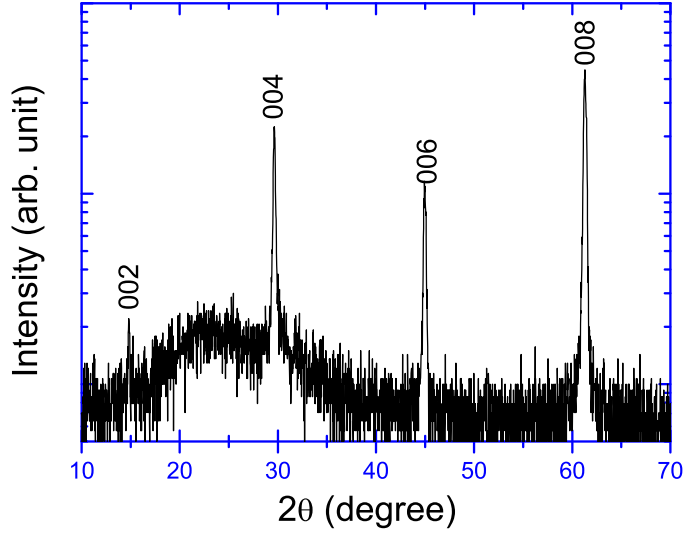


**Figure 1.** X-ray multiple diffraction pattern for  $\text{EuFe}_2\text{As}_2$  plate-like crystals lying on the sample holder. Note that the logarithmic scale was employed for the intensity axis to verify the sample quality. The hump around  $2\theta=25^\circ$  is due to the diffractions of glass sample holder.

was raised to 1398 K in 3 hours, holding for 5 hours. The crystals were grown by slow cooling to 1223 K at a rate of 2 K/h. Finally the quartz ampoule was furnace-cooled to room temperature. Many shiny plate-like crystals with the typical size of  $1.5 \times 1.5 \times 0.1 \text{ mm}^3$  were obtained.

X-ray diffraction (XRD) was performed using a D/Max-rA diffractometer with  $\text{Cu-K}\alpha$  radiation and a graphite monochromator. Fig. 1 shows the XRD pattern of  $\text{EuFe}_2\text{As}_2$  crystals. Only  $(00l)$  reflections with even  $l$  appear, indicating that the  $c$ -axis is perpendicular to the crystal plate. The  $c$ -axis was calculated as 12.11 Å, consistent with our previous measurement using polycrystalline samples[15].

Electrical resistivity was measured using a standard four-terminal method under magnetic field up to 5 T. The dc magnetization was measured on a Quantum Design magnetic property measurement system (MPMS-5). The plate-like crystal was carefully mounted in a sample holder, so that the applied field was basically perpendicular or parallel to crystallographic  $c$ -axis. The deviation angle was estimated to be less than  $5^\circ$ .

### 3. Results and discussion

Figure 2 shows the temperature dependence of magnetic susceptibility ( $\chi$ ) of  $\text{EuFe}_2\text{As}_2$  crystals in two orientations of magnetic field. At high temperatures ( $T > 50 \text{ K}$ ), there is no difference between  $\chi_{ab}$  and  $\chi_c$ , indicating isotropic susceptibility. In the range of  $19 \text{ K} \leq T < 50 \text{ K}$ , however, a significant anisotropy in susceptibility (*e. g.*,  $\chi_{ab}/\chi_c = 1.35$  at 19 K) shows up, suggesting an anisotropic magnetic interaction. Below 19 K,  $\chi_{ab}$

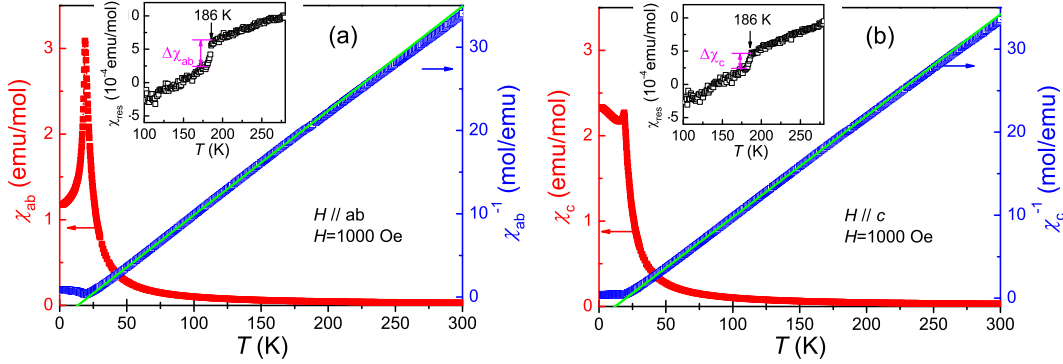


**Figure 2.** Temperature dependence of magnetic susceptibility of  $\text{EuFe}_2\text{As}_2$  crystals with the magnetic field ( $\mu_0 H = 0.1\text{T}$ ) perpendicular (a) and parallel (b) to crystallographic  $c$ -axis. The straight lines are guide to the eyes. Both insets show a drop in  $\chi$  at 186 K, after subtraction of the Curie-Weiss contribution of  $\text{Eu}^{2+}$  moments.

decreases very sharply, while  $\chi_c$  almost remains constant with decreasing temperature, indicating a Neel transition. This observation strongly suggests that the  $\text{Eu}^{2+}$  moments align within  $ab$  planes, which is different from the previous proposal by  $^{151}\text{Eu}$  Mössbauer study[19].

The high-temperature  $\chi(T)$  data follows the extended Curie-Weiss law,

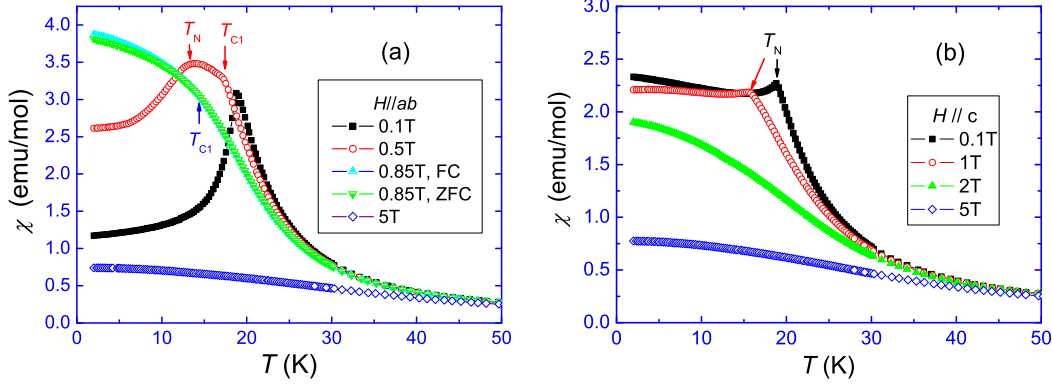
$$\chi = \chi_0 + \frac{C}{T + \theta}, \quad (1)$$

where  $\chi_0$  is the temperature-independent term of the susceptibility,  $C$  the Curie constant and  $\theta$  the Weiss temperature. The fitted parameters and the derived effective magnetic moments are listed in Table I. For both  $H \parallel c$  and  $H \parallel ab$ , the experimental value of  $\text{Eu}^{2+}$  moments is close to the theoretical value of  $g\sqrt{S(S+1)} = 7.94 \mu_B$  with  $S = 7/2$  and  $g=2$ . The Weiss temperature is negative, indicating predominately ferromagnetic interaction among  $\text{Eu}^{2+}$  spins. To reconcile the AFM ordering and the ferromagnetic interaction, and considering the enhanced  $\chi_{ab}$  just above the Neel temperature, the  $\text{Eu}^{2+}$  spins probably align ferromagnetically within  $ab$  planes, but antiferromagnetically along the  $c$ -axis (see the inset of Fig. 5). This magnetic structure of Eu sublattice resembles that of  $\text{LaMnO}_3$ , which was called  $A$ -type antiferromagnetism[20]. A more relevant example is  $\text{RNi}_2\text{B}_2\text{C}$  ( $R=\text{Pr, Dy and Ho}$ ) whose magnetic structure is also of  $A$ -type[21]. Further experiments such as neutron diffractions are needed to confirm this magnetic structure.

After subtracting the above Curie-Weiss contribution, a small drop in  $\chi$  at 186 K can be found for both field orientations. This anomaly in  $\chi$  has been identified due to the AFM SDW transition[15], though the anomaly temperature is somewhat lower than that of the polycrystalline sample.  $\Delta\chi_{ab}$  is significantly larger than  $\Delta\chi_c$ , supporting that the Fe moments align within  $ab$  planes in analogue with that in other related iron arsenides revealed by the neutron diffraction studies[12, 13]. In the SDW state,  $\text{Fe}^{2+}$  moments order antiferromagnetically with a collinear *stripe-like* spin structure.

**Table 1.** Magnetic parameters from the fitting of the high-temperature (50 K  $\sim$  180 K) susceptibility data for  $\text{EuFe}_2\text{As}_2$  crystals using Eq.(1).

Fitted Parameters	$H \parallel ab$	$H \parallel c$
$\chi_0$ (emu/mol)	-0.00022	-0.00082
$C$ (emu K/mol)	7.99	8.31
$\theta$ (K)	-21.4	-19.7
$\mu_{eff}$ ( $\mu_B$ /f.u.)	7.97	8.13

**Figure 3.** Temperature dependence of magnetic susceptibility of  $\text{EuFe}_2\text{As}_2$  crystals under various magnetic fields. The magnetic field is perpendicular (a) and parallel (b) to crystallographic  $c$ -axis.

Thus, the coupling between  $\text{Eu}^{2+}$  and  $\text{Fe}^{2+}$  moments would be geometrically frustrated. Besides, the energy scale of AFM coupling of  $\text{Fe}^{2+}$  moments is estimated to be much higher than the AFM interlayer coupling of  $\text{Eu}^{2+}$  moments. Therefore, the magnetic coupling between  $\text{Eu}^{2+}$  and  $\text{Fe}^{2+}$  moments is negligible in the following discussion.

$A$ -type antiferromagnetism often undergoes metamagnetic transition under strong magnetic field because of relatively weak interlayer AFM coupling. Fig. 3 shows the  $\chi(T)$  curves under various magnetic fields. At low magnetic field of  $\mu_0 H = 0.1\text{T}$ , AFM transition takes place at 19 K. For  $\mu_0 H_{\parallel ab} = 0.5\text{T}$ , however, successive magnetic transitions were observed. First, a kink in  $\chi$  appears at  $T_{C1} = 17\text{K}$ . Then,  $\chi$  starts to drop below  $T_N = 13\text{K}$ . At lower temperatures down to 2 K, there exists impressively large residual susceptibility. When  $\mu_0 H_{\parallel ab}$  is increased to 0.85 T, only one magnetic transition can be distinguished. The transition has small magnetic hysteresis, suggesting a kind of ferromagnetism. For  $H \parallel c$ , the Neel temperature is decreased by the applied fields for  $\mu_0 H_{\parallel c} < 2\text{T}$ . When  $\mu_0 H_{\parallel c} \geq 2\text{T}$ , the AFM transition was suppressed.

Figure 4 shows the field-dependent magnetization for  $\text{EuFe}_2\text{As}_2$  crystals at various temperatures. At 50 K, which is well above the Neel temperature  $T_N$ , the  $M(H)$  curve is essentially linear. When the temperature is close to  $T_N$ , a strong non-linearity in magnetization can be seen. Below  $T_N$ ,  $M_{ab}$  first increases almost linearly, then increases abruptly to a certain value (depending on temperature), finally continues to increase to

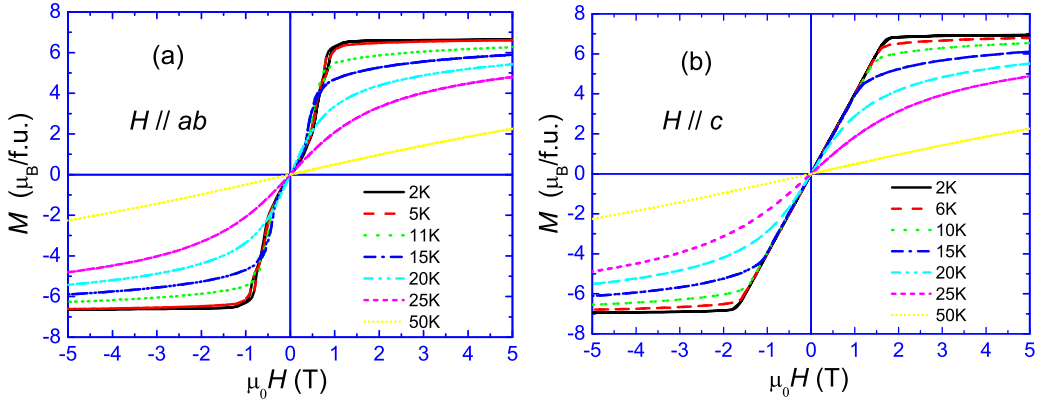


**Figure 4.** Magnetic field dependence of magnetization of  $\text{EuFe}_2\text{As}_2$  crystals with the field perpendicular (a) and parallel (b) to crystallographic  $c$ -axis.

a saturated value. Small magnetic hysteresis was identified. In the case of  $M_c$ , no such step-like magnetization behavior with magnetic hysteresis was observed. At 2 K, for example,  $M_c$  increases linearly to  $7.0 \mu_B/\text{f.u.}$  at  $\mu_0 H = 1.7$  T, then keeps at this value of saturated  $\text{Eu}^{2+}$  moments ( $M_{sat} = gS = 7.0 \mu_B/\text{f.u.}$  for  $g=2$  and  $S=7/2$ ) for higher fields. The linear field dependence of  $M_c$  is consistent with spin re-orientation, since applied field rotates the moment gradually from  $\perp c$  to  $\parallel c$ .

To analyze the complex magnetization for  $H \parallel ab$ , an expanded plot is shown in Fig. 5. The linear increase in  $M_{ab}$  below 0.45 T probably corresponds to spin re-orientation. In the field range of  $0.5 \text{ T} < \mu_0 H < 0.7 \text{ T}$ ,  $M_{ab}$  increases rapidly to  $4.4 \mu_B/\text{f.u.}$  Because of the small magnetic hysteresis, the rapid increase in  $M$  above 0.45 T is unlikely due to a spin-flop transition, and we ascribe it to a metamagnetic transition. For  $0.7 \text{ T} < \mu_0 H < 1.0 \text{ T}$ , another ferromagnetic loop can be seen.  $M_{ab}$  finally saturates to  $6.6 \mu_B/\text{f.u.}$  above 1.0 T. The saturated moment is a little smaller than the expected value of  $7.0 \mu_B/\text{f.u.}$ , which is possibly due to the crystal field effect. It is noted that the intermediate magnetization of  $4.4 \mu_B/\text{f.u.}$  is just  $2/3$  of the saturated one. Therefore, we propose a possible configuration for the intermediate metamagnetic (MM) state: In every six sheets of  $\text{Eu}^{2+}$ , five of them have the moment parallel to the external field, and the remained one has the moment antiparallel to the applied field. We note that similar MM phases were found in  $\text{RNi}_2\text{B}_2\text{C}$  system[22].

Figure 6 shows the isothermal in-plane resistance ( $R$ ) under the applied field perpendicular or parallel to the crystallographic  $c$ -axis. At 20 K, which is very close to  $T_N$ , the resistance decreases gradually at low fields, and then almost remains unchanged under higher fields. The negative magnetoresistance (MR) is ascribed to the reduction of spin disorder scattering, since the paramagnetic  $\text{Eu}^{2+}$  spins tend to align along the external magnetic field. At the temperature far below the  $T_N$  (e.g., at 2 K) in which  $\text{Eu}^{2+}$  spins order antiferromagnetically, the resistance first decreases to a minimum, then increases almost linearly. The turning point at  $H_{C3}$  corresponds to the onset of the magnetic saturation in  $M(H)$  curves. The negative MR below  $H_{C3}$  suggests that the

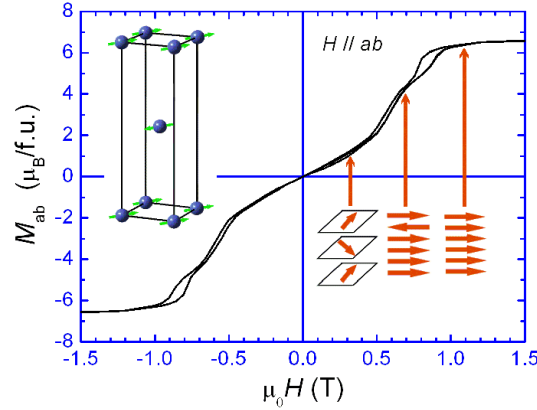


**Figure 5.** Expanded  $M - H$  plot for  $H \parallel ab$  at 2 K. The insets give the possible magnetic structure at zero field (upper left, each ball represents Eu atom with spin  $7/2$ ), and the configuration of magnetic polarization (lower right, each arrow represents the magnetic moment in a  $\text{Eu}^{2+}$  sheet).

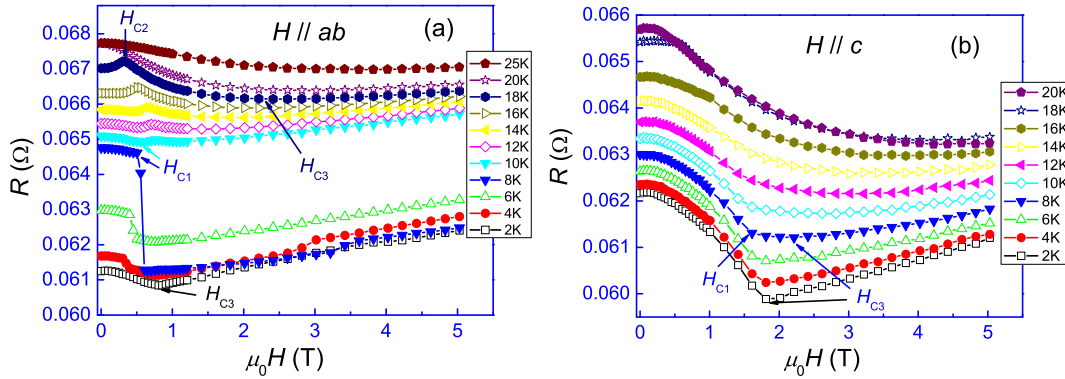


**Figure 6.** Isothermal in-plane resistance as a function of magnetic field for  $\text{EuFe}_2\text{As}_2$  crystals. The applied field is perpendicular (a) or parallel (b) to the crystallographic  $c$ -axis.

AFM-ordered  $\text{Eu}^{2+}$  spins scatter the charge transport in FeAs layers, similar to the well known giant magnetoresistance observed in magnetic multilayers[23]. The increase of MR above  $H_{C3}$  (where  $\text{Eu}^{2+}$  spins order ferromagnetically) reflects the intrinsic property of the SDW state. In fact, positive MR was observed at low temperature for  $\text{LaOFeAs}$ , which was explained in terms of the suppression of SDW order by external magnetic field[24].

The  $R(H)$  curves with  $H \parallel ab$  are shown to be more complicated. For clearness, the expanded  $R(H)$  curves are presented in Fig. 7. At the temperature slightly higher than  $T_N=19$  K,  $R$  decreases gradually with the applied field until  $R$  reaches a minimum. Since the reduction of spin-disorder scattering by external fields leads to negative MR, on the other hand, the suppression of Fe-SDW by the fields results in positive MR, the minimum of  $R$  corresponds to the ferromagnetic alignment of  $\text{Eu}^{2+}$  spins at  $H=H_{C3}$ .

At the temperature range of  $10 \text{ K} \leq T \leq 18 \text{ K}$ ,  $R(H)$  shows a peak below

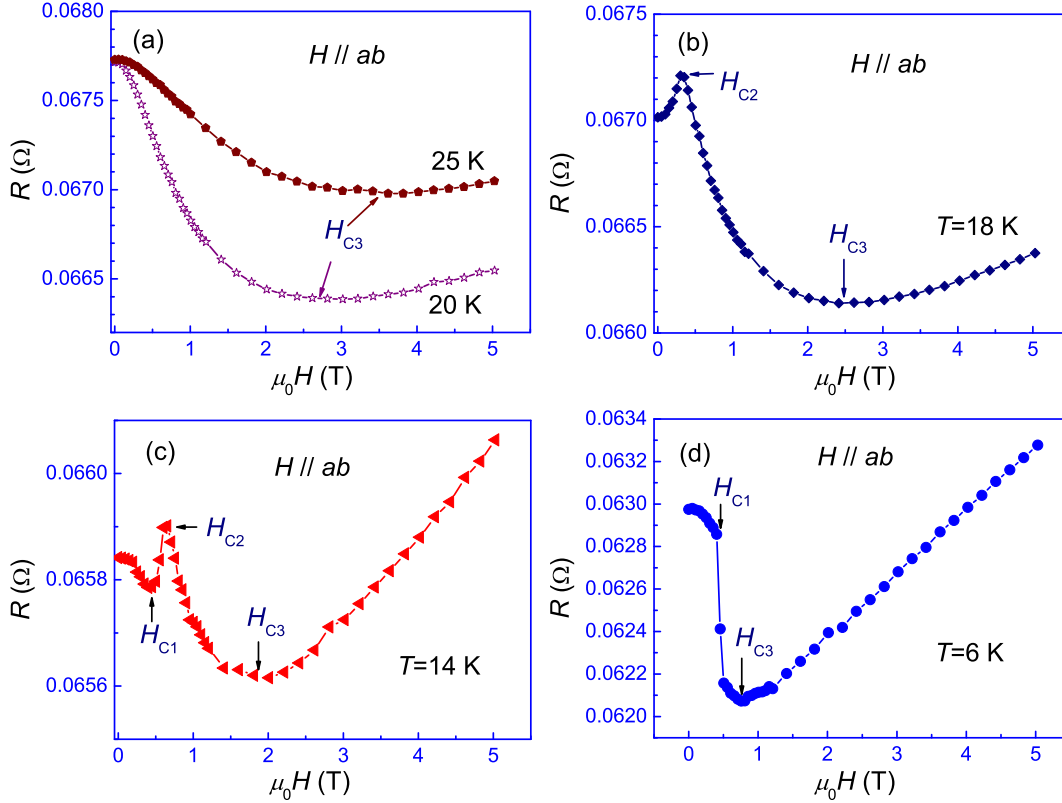


**Figure 7.** Expanded  $R_{ab}(H)$  curves with magnetic field parallel to  $ab$  planes at some representative temperatures for  $\text{EuFe}_2\text{As}_2$  crystals.

$\mu_0 H_{\parallel ab} = 1.0$  T. This high MR at  $H_{C2}$  suggests the spin disorder state (paramagnetic) of  $\text{Eu}^{2+}$  spins. Because the peak corresponds to the centre of magnetic hysteresis in the  $M(H)$  curves, the increase of  $R$  below  $H_{C2}$  is probably due to the destruction of ferromagnetic-like order of  $\text{Eu}^{2+}$  spins. On the other hand, the spin-reorientation of AFM phase causes the decrease of  $R$ . Therefore, another minimum of  $R$  appears at  $H_{C1}$ . For  $8 \text{ K} \leq T \leq 4 \text{ K}$ , a sharp drop in  $R$  was observed, which is due to the formation of a certain AFM configuration like we proposed above.

The above data allow us to draw magnetic phase diagrams, as shown in Fig. 8. For  $H \parallel c$ , one sees an AFM region at low temperatures and low fields, in which spin re-orientation dominates. Stronger fields lead to ferromagnetic (FM) state showing saturated magnetic moments. The other region is paramagnetic (PM) at elevated temperatures in which the  $\text{Eu}^{2+}$  moments are aligned to some extent by the external fields. For  $H \parallel ab$ , the external fields lead to spin reversal as well as spin re-orientation. Apart from AFM, FM and PM phases, there is an additional MM region.

#### 4. Conclusion

To summarize, the property of AFM order of  $\text{Eu}^{2+}$  spins and the evolution of the magnetic ordering under various magnetic fields were studied by the measurements



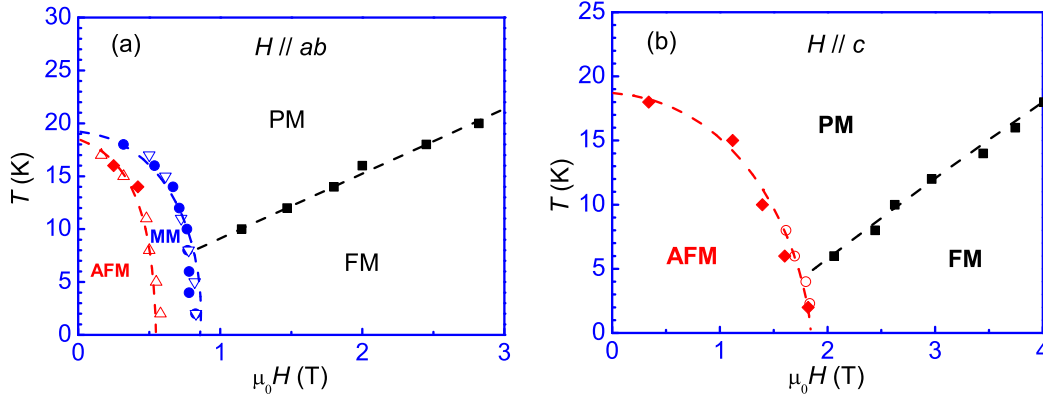


**Figure 8.** Tentative magnetic phase diagrams for  $\text{EuFe}_2\text{As}_2$ . The applied field is perpendicular (a) or parallel (b) to the crystallographic  $c$ -axis. The open and filled symbols are from  $M(H)$  and  $R(H)$  measurements, respectively. The dashed lines are guides to the eyes.

of magnetization and magnetoresistance using  $\text{EuFe}_2\text{As}_2$  single crystal samples. The result suggests that the magnetic structure for  $\text{Eu}^{2+}$  spins is of  $A$ -type. Under external magnetic fields with  $H \parallel ab$  or  $H \parallel c$ , the  $\text{Eu}^{2+}$  moments undergo spin-reorientation and/or spin-reversal transition depending on the relative orientations between  $\text{Eu}^{2+}$  moments and magnetic field. The magnetoresistance reflects the charge carrier scattering by the  $\text{Eu}^{2+}$  moments. The electrical conduction of FeAs layers was found to be related to the magnetic state of Eu layers. Our preliminary result of Ni-doping[25] in  $\text{EuFe}_2\text{As}_2$  suggests that the magnetic state of Eu layers even influences the appearance of superconductivity.

## Acknowledgement

This work is supported by the National Basic Research Program of China (Contracts Nos. 2006CB601003 and 2007CB925001) and the PCSIRT of the Ministry of Education of China (Contract No. IRT0754).

## References

- [1] Kamihara Y, Watanabe T, Hirano M, and Hosono H 2008 *J. Am. Chem. Soc.* **130** 3296
- [2] Chen X H, Wu T, Wu G, Liu R H, Chen H, and Fang D F 2008 *Nature* **453** 761
- [3] Chen G F, Li Z, Wu D, Li G, Hu W Z, Dong J, Zheng P, Luo J L, and Wang N L 2008 *Phys. Rev. Lett.* **100** 247002
- [4] Ren Z A, Lu W, Yang J, Yi W, Shen X L, Zheng C, Che G C, Dong X L, Sun L L, Zhou F and Zhao Z X *et al.* 2008 *Chin. Phys. Lett.* **25** 2215
- [5] Kito H, Eisaki H and Iyo A 2008 *J. Phys. Soc. Jpn.* **77** 063707
- [6] Wang C, Li L J, Chi S, Zhu Z W, Ren Z, Li Y K, Wang Y T, Lin X, Luo Y K, Jiang S, Xu X F, Cao G H, and Xu Z A 2008 *Europhys. Lett.* **83** 67006
- [7] Rotter M, Tegel M, and Johrendt D 2008 *Phys. Rev. Lett.* **101** 107006; Ni N, Budko S L, Kreyssig

- A, Nandi S, Rustan G E, Goldman A I, Gupta S, Corbett J D, Kracher A, and Canfield P C 2008 *Phys. Rev. B* **78** 014507
- [8] Chen G F, Li Z, Li G, Hu W Z, Dong J, Zhang X D, Zheng P, Wang N L, and Luo J L 2008 *Chin. Phys. Lett.* **25** 3403; Sasmal K, Lv B, Lorenz B, Guloy A, Chen F, Xue Y, and Chu C W 2008 *Phys. Rev. Lett.* **101** 107007
- [9] Wu G, Liu R H, Chen H, Yan Y J, Wu T, Xie Y L, Ying J J, Wang X F, Fang D F, and Chen X H 2008 *Europhys. Lett.* **84** 27010
- [10] Wu G, Chen H, Wu T, Xie Y L, Yan Y J, Liu R H, Wang X F, Ying J J, and Chen X H 2008 *J. Phys: Condens. Matter* **20** 422201
- [11] Wang X C, Liu Q Q, Lv Y X, Gao W B, Yang L X, Yu R C, Li F Y, and Jin C Q 2008 *Preprint* 0806.4688
- [12] de la Cruz C, Huang Q, Lynn J W, Li J, Ratcliff II W, Mook H A, Chen G F, Luo J L, Wang N L, and Dai P C 2008 *Nature* **453** 899
- [13] Huang Q, Qiu Y, Bao W, Lynn J W, Green M A, Gasparovic Y C, Wu T, Wu G, and Chen X H 2008 *Preprint* 0806.2776
- [14] Marchand R, Jeitschko W 1978 *J. Solid State Chem.* **24** 351
- [15] Ren Z, Zhu Z W, Jiang S, Xu X F, Tao Q, Wang C, Feng C M, Cao G H, and Xu Z A 2008 *Phys. Rev. B* **78** 052501
- [16] Jeevan H S, Hossain Z, Geibel C, and Gegenwart P 2008 *Phys. Rev. B* **78** 092406
- [17] Qi Y P, Gao Z S, Wang L, Wang D L, Zhang X P, Ma Y W 2008 *Preprint* 0807.3293
- [18] Wang X F, Wu T, Wu G, Chen H, Xie Y L, Ying J J, Yan Y J, Liu R H, and Chen X H 2008 *Preprint* 0806.2452
- [19] Raffius H, Mörsen E, Mosel B D, Müller Warmuth W, Jeitschko W, Terbüchte L, Vomhof T, 1993 *J. Phys. Chem. Solids* **54** 135
- [20] Wollan E O and Koehler W C 1955 *Phys. Rev.* **100** 545
- [21] Lynn J W, Skanthakumar S, Huang Q, Sinha S K, Hossain Z, Gupta L C, Nagarajan R, and Godart C 1997 *Phys. Rev. B* **55** 6584
- [22] Detlefs C, Bourdarot F, Burlet P, Dervenagas P, Budko S L and Canfield P C 2000 *Phys. Rev. B* **61** R14916
- [23] Baibich M N, Brotp J M, Fert A, Nguyen Van Dau F, Petroff F, Etienne P, Creuzet G, Friederich A and Chazelas J 1988 *Phys. Rev. Lett.* **61** 2472
- [24] Dong J, Zhang H J, Xu G, Li Z, Li G, Hu W Z, Wu D, Chen G F, Dai X, Luo J L, Fang Z, and Wang N L 2008 *Europhys. Lett.* **83** 27006
- [25] Ren Z, Lin X, Tao Q, Jiang S, Zhu Z W, Wang C, Cao G H, and Xu Z A 2008 *Preprint* 0810.2595